Functional Gap Junctions in the Schwann Cell Myelin Sheath

Rita J. Balice-Gordon,* Linda J. Bone,‡ and Steven S. Scherer‡

*Department of Neuroscience and ‡Department of Neurology, The University of Pennsylvania School of Medicine, Philadelphia, Pennsylvania 19104-6074

Abstract. The Schwann cell myelin sheath is a multilamellar structure with distinct structural domains in which different proteins are localized. Intracellular dye injection and video microscopy were used to show that functional gap junctions are present within the myelin sheath that allow small molecules to diffuse between the adaxonal and perinuclear Schwann cell cytoplasm. Gap junctions are localized to periodic interruptions in the compact myelin called Schmidt–Lanterman incisures and to paranodes; these regions contain at least one gap junction protein, connexin32 (Cx32). The radial diffusion of low molecular weight dyes across the myelin sheath was not interrupted in myelinating Schwann cells from *cx32*-null mice, indicating that other connexins participate in forming gap junctions in these cells. Owing to the unique geometry of myelinating Schwann cells, a gap junction-mediated radial pathway may be essential for rapid diffusion between the adaxonal and perinuclear cytoplasm, since this radial pathway is approximately one million times faster than the circumferential pathway.

Key words: myelin • gap junctions • glia • connexin • neuropathy • Schwann cell

THE myelin sheath is a multilamellar structure that ensheathes axons in the peripheral nervous system (PNS)[1] and central nervous system of vertebrates, increasing axonal conduction velocity by restricting the depolarizing ionic fluxes that generate action potentials to nodes of Ranvier (Salzer, 1997). In the PNS, Schwann cells make the myelin sheath, which is composed of two distinct domains, compact myelin and noncompact myelin, each containing distinct proteins. Compact myelin contains protein zero, peripheral myelin protein of 22 kD, and myelin basic protein. Noncompact myelin, found in paranodes and in periodic interruptions in the compact myelin called Schmidt–Lanterman incisures, contains myelin-associated glycoprotein (MAG), the gap junction protein connexin32 (Cx32, also known as β1 connexin), and E-cadherin (Scherer, 1996). E-cadherin is localized to adherens junctions by immunoelectron microscopy (Fannon et al., 1995), and the localization of Cx32 coincides with the location of gap junction-like collections of particles by freeze fracture electron microscopy (Sandri et al., 1982; Tetzlaff, 1982). Although adherens junctions and gap junctions are typically found between neighboring cells, in the myelin sheath they join adjacent layers. These radially arrayed junctions are thus unique examples of how reflexive junctions (Herr and Heidger, 1978; Majack and Larsen, 1980; Rumessen et al., 1982) may serve a functional role.

In addition to these molecular specializations, there has been a renewed interest in the electrophysiological functions of myelinating Schwann cells. Although myelinating Schwann cells are typically characterized as providing relatively static axonal insulation, they also possess several kinds of ion channels (Chiu, 1991; Sontheimer, 1994; Mi et al., 1995, 1996), and respond to ion fluxes that accompany axonal action potentials (Lev-Ram and Ellisman, 1995). Moreover, when their contact with axons is disrupted, they develop voltage-dependent sodium and potassium conductances (Chiu, 1991), may become coupled by gap junctions (Chandross et al., 1996*a*; Tetzlaff, 1982), and extend networks of processes that axons use as substrates for regeneration (Reynolds and Woolf, 1992; Son and Thompson, 1995*a*,*b*).

The finding that Cx32 is localized to the incisures and paranodes, where putative gap junctions have been observed, led us to investigate whether incisures and paranodes have functional gap junctions. Such gap junctions could promote intracellular communication, since reflex-

Address all correspondence to R.J. Balice-Gordon, Department of Neuroscience, University of Pennsylvania School of Medicine, 215 Stemmler Hall, Philadelphia, PA 19104-6074. Tel.: (215) 898-1037. Fax: (215) 573-9050. E-mail: rbaliceg@mail.med.upenn.edu

A portion of these results has appeared in abstract form (Bone, L.J., S.S. Scherer, and R.J. Balice-Gordon. 1996. The role of the gap junction protein connexin32 in myelinating Schwann cells. *Soc. Neurosa Abstracts*. 22:1981).

1. *Abbreviations used in this paper*: AGA, 18-α-glycerrhetinic acid; CMTX, X-linked Charcot-Marie-Tooth disease; Cx32, connexin32; MAG, myelin-associated glycoprotein; PNS, peripheral nervous system; SIT, silicon-intensified target.

ive gap junctions could provide a radial pathway directly across the myelin sheath. This radial pathway could facilitate the spatial buffering of extracellular potassium during action potential activity (Orkand et al., 1966) and the communication between the adaxonal cytoplasm and the nucleus. We used intracellular dye injection into living, myelinating Schwann cells ensheathing axons and video microscopy to demonstrate that functional, reflexive gap junctions mediate a radial pathway for diffusion of small molecules across the myelin sheath at incisures and paranodes. This radial pathway was also present in myelinating Schwann cells from *cx32*-null mice, indicating that other connexins participate in forming reflexive gap junctions. The gap junction-mediated radial pathway may be important for rapid diffusion between the adaxonal and perinuclear cytoplasm that would take approximately one million times longer via a circumferential route.

Materials and Methods

Preparation of Teased Sciatic Nerve Fibers

Young adult (7- or 8-wk-old) mice were anesthetized with CO_2 and killed by cervical dislocation. Mouse sciatic nerves were removed and incubated in an ice-cold, oxygenated, buffered salt solution (137 mM NaCl, 5 mM KCl, 2 mM $CaCl_2$, 1 mM $MgCl_2$, 29 mM $NaHCO_3$, 1 mM $NaHa_2PO_4$, 11 mM glucose, pH 7.4, at room temperature). To promote the adhesion of teased fibers and facilitate location of injected fibers after immunohistochemical processing, fibers were teased into small bundles on ~1 × 1-mm grids inscribed on tissue culture dishes with a scalpel blade. Nuclei were visualized after staining with 0.1 μg/ml bis-benzamide (Hoechst; Molecular Probes Inc., Eugene, OR) in Ringer's for at least 5 min. Incisures and paranodes were visualized with polarized light, since they are isotropic and can be differentiated from anisotrophic compact myelin.

In some experiments, nerve fibers were teased from rat and frog sciatic nerves. Rats were anesthetized as described above. Frogs were immersed in ice for 3–5 min and pithed before dissection of the sciatic nerve. In the case of frog sciatic nerve, fibers were incubated in a buffered salt solution, 115 mM NaCl, 2.5 mM KCl, 1.8 mM $CaCl_2$, 1 mM $MgCl_2$, 2.15 mM Na_2HPO_4, 0.85 mM NaH_2PO_4, pH 7.1–7.2.

Injection of Sciatic Nerve Fibers

The perinuclear region identified by bis-benzamide staining was impaled with intracellular electrodes which were pulled from borosilicate glass with filament with fine tapers (1-μm shank size near tip; R = 40–60 megaOhms measured in 3 M K-acetate). For injection, 5 mg/ml 5,6-carboxyfluorescein (molecular weight of 376 kD; Molecular Probes, Inc.), Lucifer yellow (molecular weight of 457 kD; Molecular Probes, Inc.), 10% neurobiotin (molecular weight of 323 kD; Vector Labs, Inc., Burlingame, CA), or 3,000 Da rhodamine dextran (Sigma Chemical Co., St. Louis, MO) were solubilized in a buffered intracellular injection solution consisting of 140 mM K-acetate, 10 mM Hepes buffer, and 5 mM EDTA, pH 7.4. In some experiments, 5,6-carboxyfluorescein and neurobiotin were coinjected.

Current injection (5–10 nA, 100-ms pulses, 2 Hz for 2–3 min) was used to iontophoretically inject dye into the perinuclear cytoplasm (model Axoprobe 1A; Axon Instruments, Inc., Foster City, CA). Injections were considered to be successful if a resting potential below 4 mV and rapid longitudinal dye diffusion were observed; ~60–70% of injected fibers met this criteria, and only these fibers were analyzed further.

Pressure injection was used to inject large molecular mass dyes because iontophoretic injection was unreliable. Pressure injection was delivered at 5–40 psi, 250-ms pulses at 2–3 Hz for 0.5–2 min using a homemade picospritzer and continuous visual observation. Dye passage through the high resistance electrodes needed to impale Schwann cells was difficult. Many injections were judged to have failed, either because dye did not diffuse beyond the nuclear area, or because the electrodes clogged during the injection. These were not analyzed further.

Neurobiotin Histochemistry and Immunohistochemistry of Injected Sciatic Nerve Fibers

After some injections, fibers were stained immunohistochemically for MAG after fixation in 4% paraformaldehyde and permeabilization with acid alcohol for 10 min. Fibers were blocked in 5% fish skin gelatin and 0.1% Triton X-100 and then incubated with a polyclonal rabbit anti-MAG antiserum (Pedraza et al., 1990), followed by rhodamine-conjugated donkey anti–rabbit secondary antibody as previously described (Scherer et al., 1995). The resulting staining pattern was evaluated using epifluorescence or confocal microscopy. To ascertain the localization of Cx32, we similarly immunostained adult rat teased fibers (fixed in Zamboni's fixative [Zamboni, L., and C. de Martino. 1967. *J. Cell Biol.* 35:148a] for 30 min) with a monoclonal antibody for Cx32 (7C6.C7; Li et al., 1997) and a rabbit antiserum against E-cadherin (Fannon et al., 1995).

Injected neurobiotin was visualized after fixation in 4% paraformaldehyde and permeabilization with acid alcohol. Fibers were blocked in 5% fish skin gelatin and 0.1% Triton X-100, labeled with 50 μg/ml rhodamine-conjugated strepavidin (Sigma Chemical Co.). Injected Schwann cells were then relocated using the etched grid as a guide (see Fig. 1, *C* and *D*) and imaged using confocal microscopy.

In some experiments, the viability of fibers was also evaluated by a live/dead assay according to the manufacturer's instructions (Molecular Probes, Inc.). When viewed with the appropriate fluorescence optics, this technique stains living cells green (because they internalize and process calcein AM ester) but not red (because they exclude ethidium bromide homodimer from the nucleus).

Video Microscopy

In most experiments, dye diffusion was recorded with a 40×, 0.75 n.a., long-working distance tapered water immersion objective (Achroplan 40; Carl Zeiss, Inc., Thornwood, NY), a modified Leica epifluorescence microscope (model DMRX; Leica USA, Deerfield, IL) (Balice-Gordon, 1998) with a low-light level silicon-intensified target (SIT) video camera (model VE1000SIT; Dage-MTI, Michigan City, IN) and a PC-based image processing system (MetaMorph; Universal Imaging Corp., West Chester, PA). The software used for acquisition automatically noted the time each frame was acquired. The path of dye diffusion was monitored visually continuously during injection; images were acquired at variable intervals during the injection. In some experiments, images were acquired digitally at video rates (30 frames/s) during the first few minutes after injection, and a few experiments were also recorded onto videotape.

Confocal Microscopy

After injection and imaging, some living fibers were analyzed using laser scanning confocal microscopy (model TCS4D; Leica USA) after being relocated on the etched grid. This analysis typically took place 10–60 min after the injection was completed. Fibers were imaged using 40×, 1.0 n.a. and/or 100×, 1.4 n.a. oil immersion objectives. Z series were taken through the entire fiber at near the limit of resolution. The single confocal planes near the middle of the z series that contained the widest width of axon diameter in addition to the myelin sheath were analyzed for the pattern of dye diffusion. Some fibers were subsequently fixed and processed for neurobiotin staining and/or immunohistochemistry and then analyzed again by confocal microscopy.

Image Analysis

Images were archived onto magneto-optical disks and printed using a dye sublimation printer (model Phaser 440; Tektronix, Wilsonville, OR). The pattern of dye distribution after injection was analyzed in single light microscopic or confocal images by mapping the intensities of pixels in a line 10–20 pixels wide, perpendicular to the long axis of the fiber (MetaMorph software; Universal Imaging Corp.). At least three regions were sampled in each image. In fibers judged to have been successfully injected (see above for criteria), one of two patterns was observed in each fiber analyzed, regardless of image contrast enhancement or the absolute intensity of labeling. In some cases, the line intensity histogram included a pair of single peaks separated by 8–12 μm. In other cases, the line intensity histogram included one or two peaks that were doublets, with each peak within the doublet separated by 1 μm or less. The distance between the doublets was compared with the distance between the outermost peak.

The rate of dye diffusion across incisures was measured from iontophoretic injection of myelinating Schwann cells from wild-type and *cx32*-

null mice, in a set of experiments in which images were acquired at 30 frames/s from the onset of injection. Due to the limited spatial and temporal resolution of light video microscopy, we could not measure the rate of diffusion within incisures per se. Instead, we analyzed video frames (2–6 frames, 33 ms apart) in which we could clearly see an incisure in the field and measure the location of the dye front before, during and after the inner collar of cytoplasm filled.

Pharmacological Blockade of Gap Junctions

Halothane, octanol, and 18-α-glycerrhetinic acid (AGA) were purchased from Sigma Chemical Co. Nerve fibers were incubated in 1–10% halothane, 1–100 μM octanol, or 1–100 μM AGA. AGA was dissolved in DMSO (100-mM stock solution) and diluted to 75 μM in oxygenated Ringer's immediately before use. Nerve fibers were incubated in AGA for 40–105 min and then were injected iontophoretically with 5,6-carboxyfluorescein and were monitored optically for 1–4 h. All values are reported as mean ± SEM.

Generation of Cx32 Mutant Mice

The generation and initial characterization of *cx32*-null (*cx32*−/− female and *cx32*Y/−) mice has been described (Nelles et al., 1996). Animals were generated from our colony at the University of Pennsylvania from two breeding pairs of *cx32*-null mice obtained from K. Willecke (University of Bonn, Bonn, Germany) (Nelles et al., 1996). Genotypes were established by PCR analysis of genomic DNA isolated from tail clips (Anzini et al., 1997), and confirmed by Southern blot analysis.

Results

Intracellular Dye Injection and Imaging of Living Myelinating Schwann Cells

To determine whether a radial pathway exists across the myelin sheath, mouse sciatic nerves were removed, incubated in physiological salt solution, and then teased into small bundles. Teased fibers were stained with bis-benzamide to identify the Schwann cell perinuclear region (Fig. 1 *A*, *inset*), which contains the largest amount of Schwann cell cytoplasm (Gould and Mattingly, 1990). Large myelinated fibers were selected for injection, and the perinuclear region was impaled with a microelectrode (Fig. 1 *A*) and injected with fluorescent dyes either by iontophoresis (Fig. 1, *B* and *C*) or by pressure. The pathway of dye diffusion was monitored with epifluorescence microscopy and the location of injected fibers was mapped using a grid etched into the bottom of the injection dish (Fig. 1 *D*). In iontophoresis experiments, Schwann cell resting membrane potential was monitored during and after iontophoretic injection as an index of cell viability. Schwann cell resting membrane potentials (−12.2 ± 1.9 mV; n =33 fibers from 13 mice) were similar to those previously reported (Wilson and Chiu, 1993) and remained constant or improved during the course of the injection. Thus the dissection, injection, and imaging procedures did not seem to affect the viability of myelinating Schwann cells.

Low Molecular Mass Dyes Traverse the Myelin Sheath

Teased fibers were viewed with polarized light, revealing the locations of incisures, which are funnel-shaped, isotropic structures that interrupt the anisotropic compact myelin (Fig. 2 *A*). In some fibers, we directly demonstrated that these isotropic structures are incisures by fixing the fibers and immunostaining them for MAG, which is localized to incisures and the adaxonal surface of myelinating Schwann cells (Fig. 2 *B*). Finally, we double labeled teased fibers with antibodies against Cx32 and E-cadherin, which were colocalized at incisures and paranodes (Fig. 3). Thus, incisures can visualize in living teased fibers, and contain Cx32, MAG, and E-cadherin.

After injection of low molecular mass dyes, such as 5,6-carboxyfluorescein (376 Da), into the perinuclear region, we consistently observed a pattern of labeling similar to a pair of train tracks. Each track consisted of a double line of fluorescence, the lines separated by an unstained space that corresponded precisely to the location of compact myelin (compare Fig. 2, *A* with *C*). A similar pattern was observed when dye was injected by iontophoresis (n = 30/33 fibers from 13 mice) or by pressure (n = 35/40 fibers from 24 mice). The train track pattern was observed in images that included the widest diameter of the axon, usually midway through the depth of the myelinated fiber. Cytoplasmic labeling was seen in planes above and below the planes containing the train track pattern (Fig. 2 *D*). Although dye diffusion was usually monitored near the site of injection, in most fibers, dye also rapidly diffused to each node, filling the paranodal region. The dynamics of dye diffusion were not routinely monitored in this location due to its distance from the site of injection, which precluded the paranodes from being visualized in the same field as the site of injection. Dye was not observed to pass from Schwann cells to axons nor to cross nodes of Ranvier (Fig. 1 *C* and Fig. 2 *B*), as previously reported (Konishi, 1990; David et al., 1993; Dezawa et al., 1998).

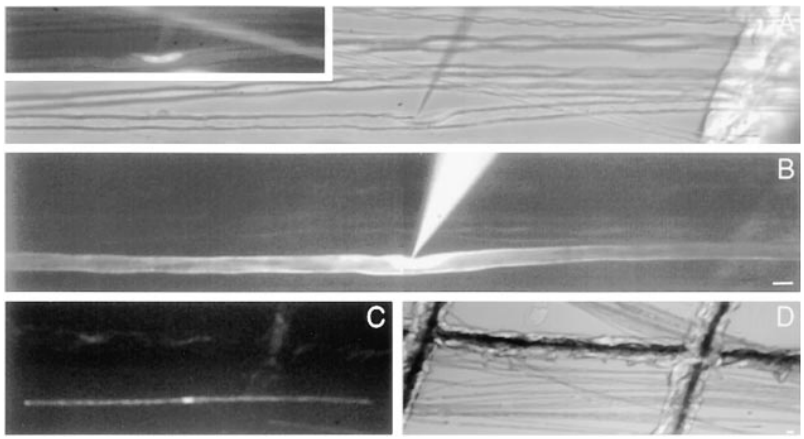

Figure 1. Dye injection into living, teased myelinated fibers from mouse sciatic nerve. Shown are images of a single fiber that was iontophoretically injected with 5,6-carboxyfluorescein. (*A*) Polarized light in combination with fluorescent bis-benzamide staining (*inset*) shows an electrode near a Schwann cell nucleus. (*B*) Diffusion of 5,6-carboxyfluorescein during iontophoretic injection. (*C*) Diffusion of dye from node to node was observed within 0.5–5 min (this image was captured at ~1 min into injection). (*D*) After imaging of dye diffusion, injected fibers were mapped at lower magnification relative to grid lines (same field as *C*) to facilitate identification for confocal microscopic analysis. Bars, 10 μm.

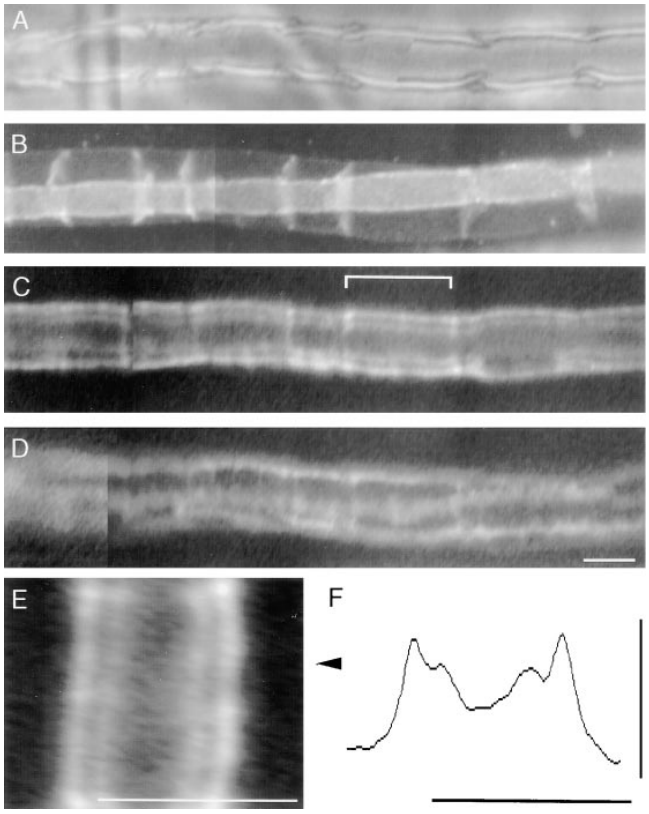

Figure 2. Dye diffusion results in labeling of adaxonal and abaxonal cytoplasm. Shown are images taken after pressure injection (40 psi, 250-ms pulses, 2 Hz for 1–3 minutes) of 5,6-carboxyfluorescein into a myelinating Schwann cell. (*A*) Schwann cell perinuclear region and incisures visualized with polarized light. (*B*) After injection, the fiber was immunostained for MAG, which is localized to incisures and colocalizes with incisures identified with polarized light. (*C*) Image taken about midway through depth of the cell shows that dye occupies the outer and inner collar of Schwann cell cytoplasm, creating a double train track pattern indicative of the radial diffusion of dye through incisures. *Bracket,* region enlarged in *E*. (*D*) Image taken at ~5 μm above the plane shown in *G* reveals fingers of cytoplasm on the surface of the cell; these are easily distinguished from the double train track pattern. (*E*) Enlargement of region indicated by *brackets* in *C*; *arrowheads* indicate position of the line across which intensity was mapped. (*F*) Histogram of intensity across line perpendicular to the long axis of the fiber at location indicated by *arrowhead*; scale is the same as in image shown in *E*. Doublet of peaks on either end of the histogram is the quantitative representation of the double train track pattern evident in the image shown in *E*. Vertical scale is 0–255 intensity levels. Bars, 10 μm.

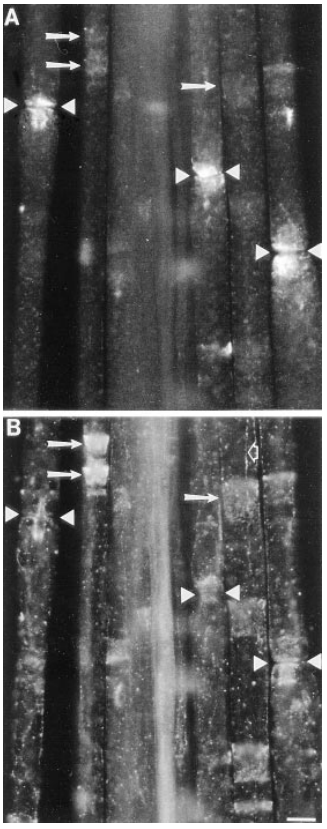

Figure 3. Cx32 and E-cadherin immunoreactivity in paranodes and incisures. Teased fibers from an adult rat sciatic nerve fixed for 30 min in Zamboni's fixative were immunostained with a monoclonal antibody against Cx32 (*A*; fluorescein optics) and a rabbit antiserum against E-cadherin (*B*; rhodamine optics). Cx32 and E-cadherin colocalize at paranodes, which flank nodes of Ranvier (*apposed arrowheads*), as well as incisures, some of which are marked (*arrows*). E-cadherin also stains mesaxons, one of which is seen in this focal plane (*open arrow*). Note that although E-cadherin and Cx32 immunoreactivity colocalize, E-cadherin staining is more pronounced at incisures, whereas Cx32 staining is more pronounced at paranodes. In addition, the subcellular distributions of E-cadherin and Cx32 immunoreactivity within paranodes appear to differ. Bar, 10 μm.

The pattern of 5,6-carboxyfluorescein filling indicates that this dye filled the cytoplasmic space on both sides of the myelin sheath. To analyze this further, we mapped the intensities of pixels in line perpendicular to the long axis of the fiber; this analysis is illustrated in each figure. In fibers injected with 5,6-carboxyfluorescein (Fig. 2 *E*), the line intensity histogram showed two peaks, each of which contained a second, inner peak (Fig. 2 *F*). The distance between the outermost peaks was 10.2 ± 0.7 μm, which corresponds to the diameter of large, myelinated fibers. The doublets were separated by 1.7 ± 0.4 μm; $n = 19$ fibers analyzed), which corresponds well to the thickness of the myelin sheath of the same fibers viewed by polarized optics (1.8 ± 0.5 μm; not significantly different, Student's *t* test). This analysis supports the idea that the myelin sheath separates the inner and outer collars of cytoplasm filled by dye. These data agree well with the thickness of the myelin sheath in adult peripheral nerve; the myelin sheath has been reported to account for nearly 40% of the total fiber diameter (Friede and Bischhausen, 1980; Berthold and Rydmark, 1995). In the present experiments, the thickness of the compartment bracketed by double train tracks was 37 ± 4% of the total fiber diameter (not significantly different, Student's *t* test).

To determine directly whether the double train track pattern of dye diffusion resulted from dye passing from the outer/abaxonal collar of Schwann cell cytoplasm to the inner/adaxonal collar of cytoplasm, the path of dye diffusion was monitored continuously during injection. Selected planes from one such sequence are shown in Fig. 4. From the onset of injection, dye spread rapidly along the myelin sheath, initially remaining within the outer/abaxonal collar near the nucleus (Fig. 4; *0 s*). In most fibers, the dye appeared to collect at nearby incisures (Fig. 4; *15 s*, *arrowhead*), partially filling the inner/adaxonal collar of cytoplasm immediately and more completely within a few seconds (Fig. 4; *30 s*, *arrow*). The dye continued to fill these compartments, with each line becoming progressively brighter in intensity (Fig. 4; *80* and *147 s*), and also spread longitudinally, usually reaching the nodes of Ranvier within a few minutes. Injections that were monitored with continuous acquisition onto videotape confirmed the above sequence of events, and, in addition, showed that

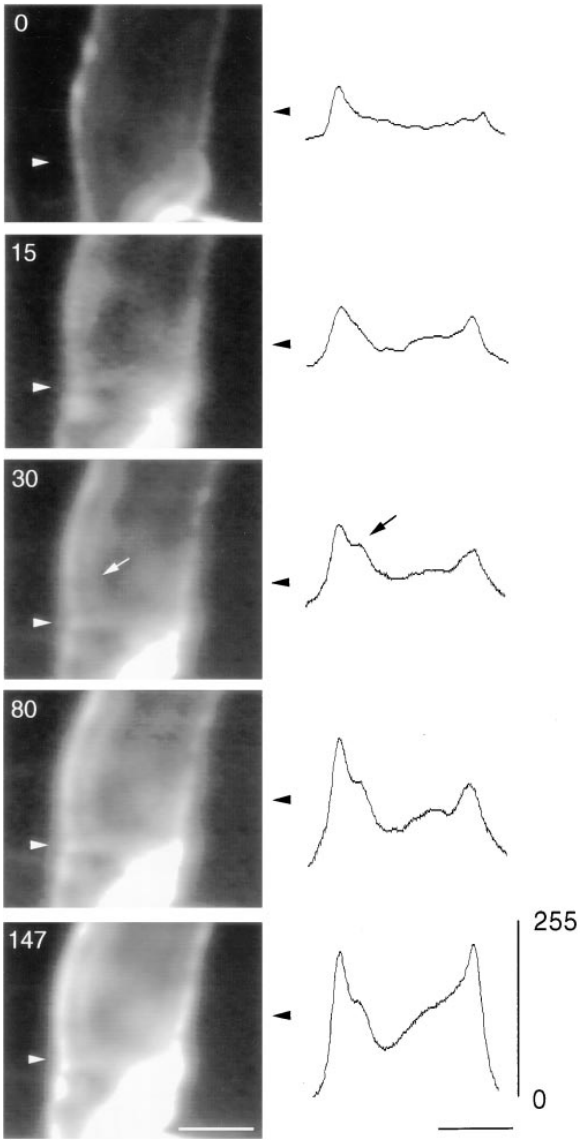

Figure 4. Rapid diffusion of 5,6-carboxyfluorescein across incisures to the inner/adaxonal collar of Schwann cell cytoplasm. *Right panels*, from the same fiber at the onset (*0 s*), and 15, 30, 80, and 147 s after the onset of iontophoretic injection. The locations of an incisure are indicated with an *arrowhead* and were confirmed by viewing the fiber with polarized light. At the onset of injection, dye immediately fills the outer collar of Schwann cell cytoplasm. By 15 s, an incisure is labeled and a faint train track is apparent on one side of the myelin sheath. The train track pattern and incisure are more apparent at 30 s. At longer times (*80* and *147 s*), more incisures become filled and the train track pattern is seen further away from the injection site, but in this case is only clearly visualized on the left side of the fiber. *Left panels,* quantitative analysis of pattern of dye distribution. The intensity of pixels in a line perpendicular to the long axis of the fiber was mapped at the position indicated by the *black arrowheads* in the corresponding photomicrograph. The light microscopic images of dye diffusion were obtained using manual gain settings of the SIT camera so that changes in the line histogram intensity mapped across the same region of the fiber over time could be compared in terms of absolute intensity (*right panels*; *0–255* intensity levels). A doublet is apparent in the *left side* of the histogram by 30 s after the onset of injection (*black arrow*; corresponding location in the 30-s image is indicated by *white arrow*). Within the doublet, the intensity of the first peak in the doublet representing the outside collar of cytoplasm and the intensity of the second peak increased over the first minutes of injection in parallel. Thus, the train track pattern of labeling is consistent with the diffusion of 5,6-carboxyfluorescein from the outer/abaxonal to the inner/adaxonal cytoplasm across incisures. Bars, 5 μm.

the incisures themselves were labeled as the dye front moved down the myelin sheath. In some fibers, including the one illustrated in Fig. 4, light microscopic images of dye diffusion were obtained using manual gain settings of the SIT camera, allowing quantitative comparisons of changes in intensity mapped across the same region of the fiber over time (Fig. 4; *right-hand panels*). This analysis confirmed that the intensity of the outer and inner cytoplasmic collars increased over time, and that the inner cytoplasmic collar filled after the outer one. Thus, the temporal sequence of the train track pattern indicates that 5,6-carboxyfluorescein diffuses from the outer/abaxonal to the inner/adaxonal cytoplasm across incisures.

The rate of dye diffusion was estimated in a subset of iontophoretic injection experiments in which images were acquired at 30 frames/s from the onset of injection ($n = 6$ fibers from 5 mice). This was accomplished by measuring the difference in the location of the dye front in consecutive images, immediately before and immediately after an incisure was filled and the train track pattern appeared. The mean rate of diffusion estimated in this way was 4.25 ± 0.49 μm/s, average ± SEM; range 2.27–6.06). We could not measure a rate of diffusion within incisures themselves owing to the limited temporal and spatial resolution of video microscopy.

We also evaluated whether other low molecular mass compounds known to cross gap junctions also filled the inner/adaxonal collar of Schwann cell cytoplasm. Fluorescence from other commonly used compounds, such as Lucifer yellow, propidium iodide, and ethidium bromide, was not as intense as that from 5,6-carboxyfluorescein, making it difficult to monitor dye movement by video microscopy. These dyes also have broad-spectrum emission that interfered with staining in other fluorescence channels. Moreover, since propidium iodide and ethidium bromide are impermeant to Cx32 channels in transfected cells (Elfgang et al., 1995), we selected Lucifer yellow and neurobiotin. Lucifer yellow injected into myelinating Schwann cells produced a double train track pattern of staining ($n = 6$ fibers from two mice; data not shown). Neurobiotin, a nonfluorescent, low-mass compound that crosses gap junctions, was coinjected iontophoretically with 5,6-carboxyfluorescein to monitor the injection (Fig. 5 *A*). The fibers were examined by confocal microscopy (Fig. 5 *B*). Evaluation of serial single confocal planes through the z axis confirmed the double train track pattern of labeling of 5,6-carboxyfluorescein, and demonstrated that this pattern was distinct from cytoplasmic labeling (Mugnaini et al., 1977; Gould and Mattingly, 1990). Fibers then were fixed, permeabilized, stained with rhodamine-conjugated strepavidin to visualize the neurobiotin, and then were then reexamined by confocal microscopy (Fig. 5 *D*; same fiber as in *A–C*), although the structure of the myelin sheath was distorted by this processing. In nine out of

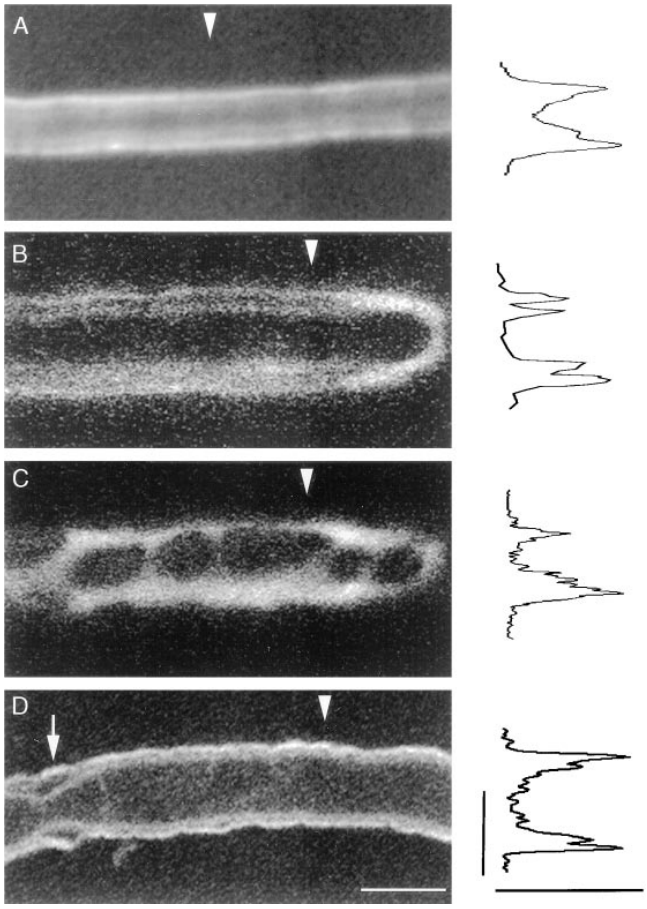

Figure 5. Injected low molecular mass compounds fill the outer/abaxonal and inner/adaxonal collars of Schwann cell cytoplasm. *A–D* are from the same fiber after injection with 5,6-carboxyfluorescein and neurobiotin. Intensity profiles are illustrated for a line perpendicular to the long axis of the fiber at the location indicated by the *white arrowhead* in each panel; the scale bar for the intensity histogram (*bottom right*) is 0–255 intensity levels. (*A*) Double line of 5,6-carboxyfluorescein observed immediately after a perinuclear injection (*left edge*). Note doublet in the peak of the intensity histogram representing each side of the fiber. (*B*) Subsequent confocal analysis of the same fiber showed a similar double train track pattern of 5,6-carboxyfluorescein within the Schwann cell along the length of the fiber. A single confocal plane, taken at near the resolution limit of the confocal microscope, midway through the depth of the cell adjacent to a node of Ranvier (*right edge*) is shown; note that this region is brighter than the double train track as there is more cytoplasm in this location. There is a doublet present in each intensity peak shown at right of photomicrograph. (*C*) A single confocal plane of ~5 μm above the plane shown in *B* demonstrates the filling of fingers of Schwann cell cytoplasm. Note absence of doublet in intensity peaks. (*D*) After confocal imaging, the same fiber was processed to visualize neurobiotin and was then reanalyzed by confocal microscopy. A single confocal plane is shown, midway through the fiber, demonstrating that neurobiotin diffusion also results in a double train track pattern, although the pattern is somewhat distorted by tissue processing. A doublet is apparent in each peak of the intensity histogram on each side of the fiber. *Arrow*, location of an incisure; visualization with polarized light confirmed this. Bars, 10 μm.

12 fibers, both 5,6-carboxyfluorescein and neurobiotin stained in a double train track pattern, indicating that both compounds filled the inner collar of Schwann cell cytoplasm. Thus, several low molecular mass compounds known to pass through gap junctions appeared to diffuse across the myelin sheath.

A small number of myelinated fibers from rats (n = 12 fibers from seven rats) and frogs (n = 8 fibers from two Rana pipiens) were also injected with 5,6-carboxyfluorescein. Incisures were present in both species. In both rats and frogs, a double train track pattern identical to that observed in mice was observed (data not shown), indicating that the incisures in these species also contain functional gap junctions.

High Molecular Mass Dyes Do Not Traverse the Myelin Sheath

Since gap junctions have been reported to have a perme-

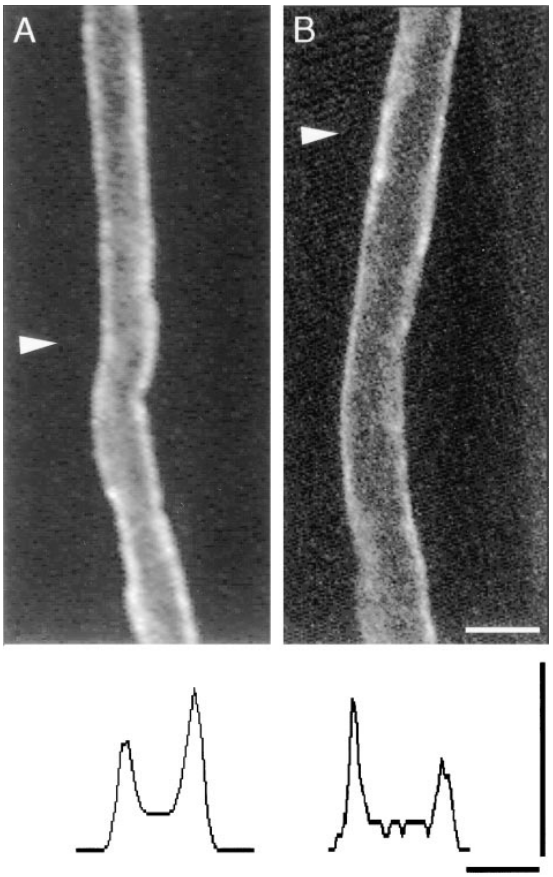

Figure 6. High molecular mass compounds do not diffuse across incisures. (*A*) Absence of a double line of dye staining 2 h after pressure injection of 3,000-Da rhodamine-conjugated dextran. (*B*) Subsequent confocal analysis of the same fiber did not reveal a double line pattern anywhere in the z projection of the cell; shown is a single confocal plane midway through the cell. Intensity profiles (marked by *white arrowhead*) illustrated at the bottom of each panel (scale, *0–255* intensity levels) confirm the absence of a doublet in any of the intensity peaks. In many cases, dye appeared to pool in the outer collar of cytoplasm near incisures but did not fill them (for example, *upper left-hand edge* of fiber above *white arrowhead*). Bars, 10 μm.

ation limit at ~1,000 Da (Bruzzone et al., 1996), we determined whether dyes of higher molecular mass would diffuse in a pattern similar to that observed with low molecular mass compounds. Pressure injection was used to inject large molecular mass dyes because iontophoretic injection was unreliable. Dye passage through the high resistance electrodes was difficult, and many injections were judged to have failed, either because dye did not diffuse beyond the perinuclear region or because the electrodes clogged during the injection (n = six out of nine injections from six mice). When 3,000-Da rhodamine-conjugated dextran was successfully injected into the perinuclear region (n = three fibers from three mice), dye spread longitudinally in a similar fashion to 5,6-carboxyfluorescein, except that fluorescence was not observed in the inner collar of Schwann cell cytoplasm. Even after allowing 1–4 h for additional diffusion (Fig. 6 *A*), dye remained confined to the outer collar of Schwann cell cytoplasm. Subsequent confocal analysis of the same fibers verified the absence of a double train track pattern of dye labeling (Fig. 6 *B*). Image analysis of intensity mapped along a line perpendicular to the long axis of injected fibers showed that no doublet in the intensity peaks was observed in any of the injected fibers (Fig. 6, *A* and *B*, *bottom*). Similar results were obtained in rats (data not shown) after injection of 3,000-Da fluorescein-conjugated dextran (n = three fibers from two rats) or 10,000-Da rhodamine-conjugated dextran (n = two fibers from one rat). Thus, low molecular mass, but not high molecular mass, compounds diffuse radially across the myelin sheath.

Dye Diffusion Across the Myelin Sheath Is Prevented by Pharmacological Blockade of Gap Junctions

To further evaluate whether functional gap junctions were present in incisures, teased nerve fibers were incubated in 1–10% halothane, 1–100 μM octanol, or 1–100 μM AGA, all of which have been shown to block gap junctions (Davidson and Baumgarten, 1988; Bruzzone et al., 1996; Goldberg et al., 1996; Goodenough et al., 1996). Schwann cell toxicity was assayed by measuring resting potential and by visually determining whether structural changes in the membrane occurred during the incubation. In some experiments, a fluorescence assay was used to evaluate cell viability, by the criteria of exclusion of ethidium bromide homodimer from the nucleus and internalization and processing of calcein AM ester which results in cytoplasmic labeling (live/dead assay, Molecular Probes, Inc.). These three criteria were used to evaluate Schwann cell viability in the course of these experiments.

Incubation in >1% halothane or >1 μM octanol rapidly induced loss of resting potential, widening of incisures, and disorganization of the Schwann cell membrane (data not shown). Teased fibers maintained in 1–100 μM AGA, however, retained their structural integrity, internalized and then processed calcein AM ester, and excluded ethidium bromide homodimer from the nucleus for more than 4 h. Thus, these concentrations of AGA did not appear to be toxic, and 75 μM AGA was used for subsequent experiments. Nerve fibers were incubated in 75 μM AGA for 40–105 min, then injected iontophoretically with 5,6-carboxyfluorescein and monitored optically for 1–4 h. In pilot

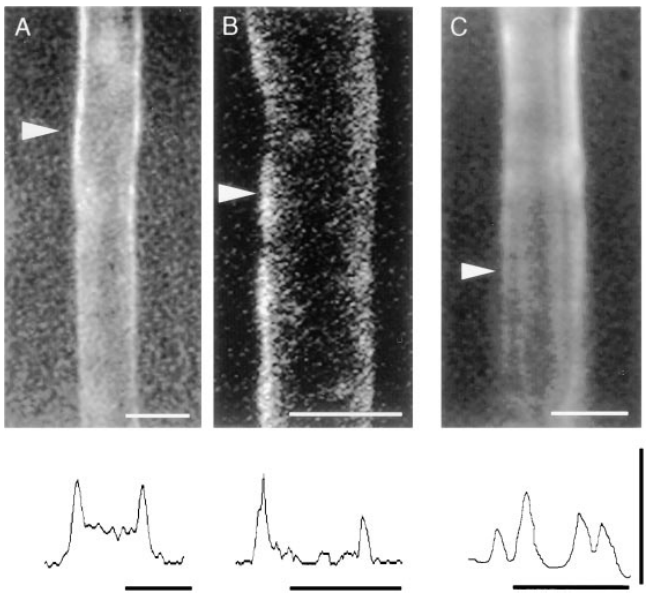

Figure 7. Pharmacologic blockade of gap junctions with AGA prevents the diffusion of 5,6-carboxyfluorescein across incisures. Intensity profiles are illustrated for each panel across a line perpendicular to the long axis of the fiber at the location indicated by the *white arrowhead* (scale, 0–255 intensity levels). (*A*) Filling of the outer, but not the inner, collar of cytoplasm 1 h after iontophoretic injection of 5,6-carboxyfluorescein after preincubation in 75 μM AGA. (*B*) Subsequent confocal analysis of 5,6-carboxyfluorescein in the same fiber shown in *A* confirmed the absence of a double train track pattern of staining; shown is a single confocal plane midway through the z projection. (*C*) Preincubation of a myelinated fiber in 0.15% DMSO for 1 h did not abolish a train track pattern of staining After injection of 5,6-carboxyfluorescein. The train track pattern is visible on the right-hand side of the fiber and also as a doublet in the intensity peak for this region. Bars, 10 μm.

experiments, we determined that 30–40 min of incubation in AGA was required to block radial dye transfer in myelinating Schwann cells. The length of time required is probably due to the geometry of the myelin sheath as well as the probable inaccessibility of putative gap junctions to bath applied AGA. In addition to retaining their structural integrity, myelinating Schwann cells incubated in AGA had resting potentials near the normal range (−8.1 ± 1.6 mV, n = 15 fibers from seven mice). Myelinating Schwann cells incubated in AGA did not have a double train track pattern after dye injection (n = six or seven fibers from five mice); the dye remained in the outer collar of cytoplasm (Fig. 7, *A* and *B*) and no doublet in the intensity histogram was observed (Fig. 7, *A* and *B*, *bottom panels*). Nerve fibers incubated in 0.15% DMSO (the carrier solution used to dissolve AGA) for a similar length of time also had resting potentials near the normal range (− 9.5 ± 1.1 mV, n = 11 fibers from six mice), but 11 out of 11 fibers showed the double train track pattern after dye diffusion, which was confirmed by the presence of a doublet in the intensity histogram on at least one side of the fiber (Fig. 7 *C*). Thus, AGA prevented dye from filling the inner collar of Schwann cell cytoplasm, suggesting that functional gap

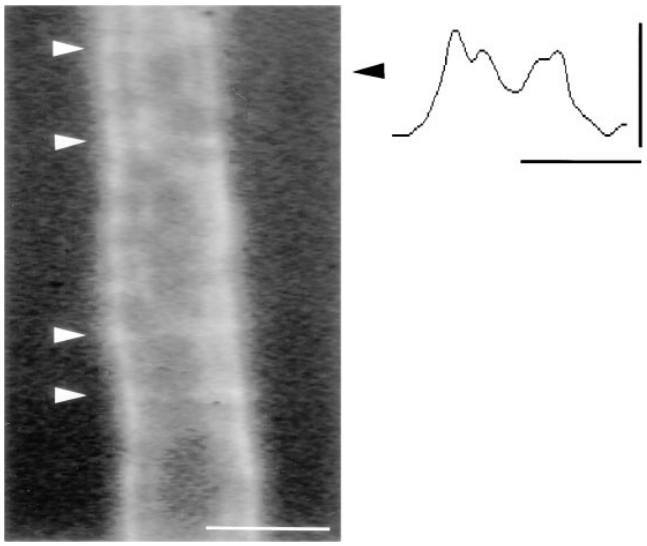

Figure 8. Evidence for functional gap junctions in the incisures of cx32-null mice. Shown is a portion of a myelinated fiber from the sciatic nerve of a cx32-null mouse after injection of 5,6-carboxyfluorescein; the location of incisures is marked with *white arrowheads*. The intensity profile is illustrated for this fiber (scale, *0–255* intensity levels) across a line perpendicular to its long axis at the location indicated by the *black arrowhead*. As in myelinating Schwann cells from wild-type mice, a train track pattern is apparent on at least one side of the axon. Bar, 10 μm.

junctions within incisures mediate the diffusion of dye into the inner collar of cytoplasm.

Dye Diffusion across the Myelin Sheath in Cx32-null Mice

Since Cx32 is the only gap junction protein known to be localized to incisures, we evaluated the possibility that Cx32 is necessary for the diffusion of small molecular mass dyes across the myelin sheath by injecting myelinating Schwann cells from *cx32*-null mice. We teased myelinated fibers from 4-mo-old mice, when few sciatic fibers are demyelinated (Anzini et al., 1997; Nelles et al., 1996; Scherer et al., 1998), avoiding any fibers that appeared abnormal, and injected them with 5,6-carboxyfluorescein by iontophoresis. When viewed with polarized light, myelinated fibers in *cx32*-null mice had incisures, which was confirmed by MAG-immunostaining (Scherer et al., 1998). The mean resting potential (−6 ± 3 mV) in myelinating Schwann cells from *cx32*-null mice was similar to that observed in wild type mice. Double train tracks of fluorescence (Fig. 8, *left*) and doublets in each peak of the line histogram analysis (Fig. 8, *right*) were observed in all of the successfully injected fibers (n = six fibers from three mice). Moreover, the mean rate of diffusion was estimated to be 4.09 ± 0.67 μm/s (n = five fibers from three mice; average ± SEM; range 2.02–7.58). This rate is not significantly different from that observed in myelinating Schwann cells from wild type mice (Student's t test). Thus, the absence of Cx32 does not appear to affect the radial pathway of dye diffusion across the myelin sheath, indicating that there are functional gap junctions in the incisures of *cx32*-null mice.

Discussion

The results of our injections provide the first functional evidence that gap junctions mediate a radial pathway of diffusion across the myelin sheath. Low molecular mass compounds diffused rapidly across the myelin sheath, from the outer/abaxonal cytoplasm to the inner/adaxonal cytoplasm, whereas high molecular mass compounds remained confined to the outer/abaxonal cytoplasm. Furthermore, the inner/adaxonal cytoplasm was not labeled after injection of low molecular mass compounds in the presence of pharmacological blockers of gap junctions. The gap junctions mediating the diffusion of low molecular mass dyes are probably localized in Schmidt–Lanterman incisures, since these structures appear to fill with 5,6-carboxyfluorescein during injections, contain Cx32-immunoreactivity (Bergoffen et al., 1993; Chandross et al., 1996*a*; Scherer

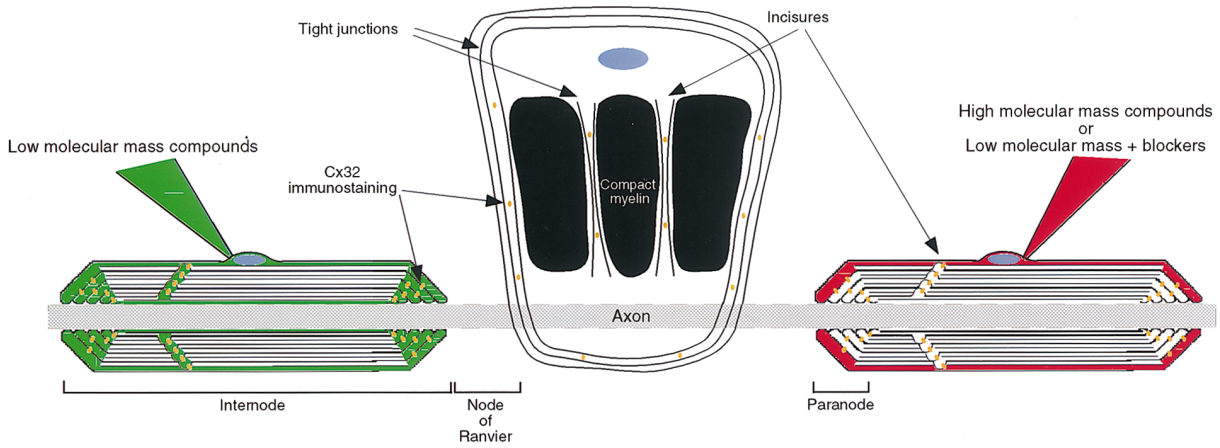

Figure 9. Schematic view of dye diffusion in myelinating Schwann cells following perinuclear dye injection. The left Schwann cell has been injected with a low molecular mass compound (e.g., 5,6-carboxyfluorescein); the right Schwann cell has been injected with a high molecular mass compound (e.g., 3,000-Da rhodamine dextran) or a low molecular mass compound in the presence of gap junction blockers. The middle Schwann cell has been unrolled to visualize regions of compact myelin, incisures and paranodes. Not to scale.

et al., 1995), and small gap junctions by freeze-fracture electron microscopy (Sandri et al., 1982; Tetzlaff, 1982).

These results are summarized in Fig. 9, which is a schematic view of dye diffusion in myelinating Schwann cells after perinuclear dye injection. One myelinating Schwann cell has been unrolled to reveal the regions of compact myelin, incisures, and paranodes. The continuous lines represent rows of tight junctions; two or more rows form a circumferential belt around the perimeter of the cell and are also found in incisures (Tetzlaff, 1978; Shinowara et al., 1980; Sandri et al., 1982; Stolinski and Breathnach, 1982). These tight junctions are probably leaky, since they are not well developed as in tight epithelia (Friend and Gilula, 1972; Claude and Goodenough, 1973). Gap junctions are depicted as ovals and are found between the rows of tight junctions. The left Schwann cell has been injected with a low molecular mass compound, which we demonstrated diffused across incisures to fill the inner collars of Schwann cell cytoplasm. This resulted in a double train track pattern whose width closely matched the width of the myelin sheath. The right Schwann cell has been injected either with a high molecular mass compound or with a low molecular mass compound in the presence of a pharmacological blocker of gap junctions. In both cases, the dye diffused within the outer collar of Schwann cell cytoplasm, but did not reach the inner collar of cytoplasm.

Functional Significance of Gap Junctions in the Myelin Sheath

The importance of gap junctions in the myelin sheath was not known until mutations in Cx32 were shown to be associated with X-linked Charcot-Marie-Tooth disease (CMTX), the eponym for dominantly inherited neuropathies (Bergoffen et al., 1993). CMTX is the second most common form of inherited demyelinating neuropathy, and more than 130 mutations in Cx32 have been described (Bone et al., 1997). The importance of Cx32 in the Schwann cell myelin sheath may owe to its unique geometry: the unrolled spiral of myelin membrane may be as long as 4 mm, whereas it is less than 4 μm in the radial dimension (Friede and Bischhausen, 1980). A radial channel through the myelin sheath would thus be roughly 1,000 times shorter than the circumferential pathway. This difference translates to a million-fold shorter diffusion time, since diffusion in a plane is proportional to the square of the distance (Berg, 1983). It is possible that this pathway may be compromised in CMTX, in which the failure of ions and small molecules to diffuse across the myelin sheath damages myelinating Schwann cells and their axons, resulting in demyelination and axonal loss (Rozear et al., 1987; Sander et al., 1998; Hahn et al., 1990).

Using video microscopy, we estimated that the rate of radial diffusion of 5,6-carboxyfluorescein across incisures was ~4 μm/s. This raises a potential problem, because if the rate of diffusion within incisures (circumferentially, within the cytoplasm) was 4 μm/s, then circumferential diffusion of 5,6-carboxyfluorescein should have been observed by 4 h in the myelinating Schwann cells that were incubated in AGA. We could not measure the rate of diffusion within the incisures, however, and this may be substantially slower than 4 μm/s. Our observation that a 3,000-kD fluorescent dye also does not reach the adaxonal cytoplasm within 4 h provides additional support for this explanation.

We observed that the myelin sheaths of *cx32*-null mice have a radial pathway for diffusion that does not appear to be significantly slower than that observed in wild-type mice. The presence of functional gap junctions in cx32-null mice indicates that myelinating Schwann cells express at least one other gap junction protein, and perhaps several. One candidate is Cx46, although Cx46 has only been shown to be expressed by denervated Schwann cells (Chandross et al., 1996*a*,*b*); whether myelinating Schwann cells also express Cx46 remains to be demonstrated. Another candidate is Cx43 (Chandross et al., 1996*a*; Scherer et al., 1995; Yoshimura et al., 1996), although this connexin has not yet been localized to incisures or paranodes. The other putative connexin(s), however, is not sufficient to preserve the functional or structural integrity of myelinating Schwann cells, as cx32-null mice develop a demyelinating neuropathy (Anzini et al., 1997; Scherer et al., 1998). This could be an indication that the gap junctions formed by other connexins are not permeant to the same molecules as gap junctions formed by Cx32 (Elfgang et al., 1995). Alternatively, Cx32 can interact with other connexins, forming heteromeric hemichannels and heterotypic channels that may have different voltage sensitivities and conductances (Bruzzone et al., 1996), so that both connexins may be required to form the proper channels in myelinating Schwann cells.

Our work provides the first demonstration of the functional importance of incisures, which are an ancient and fundamental adaptation of the myelin sheath. The gap junction plaques observed within incisures and paranodes may play a functional role in intracellular communication. Because of the unique geometry of myelinating Schwann cells, reflexive gap junctions across the myelin sheath are likely to be important for communication between the adaxonal cytoplasm and nucleus. In the absence of Cx32, intracellular communication mediated by the remaining gap junction proteins may be compromised, leading to demyelination and axonal damage.

We thank K. Fischbeck, M.P. Nusbaum (both from University of Pennsylvania School of Medicine, Philadelphia, PA), and M.J. Pinter (Allegheny University of the Health Sciences, Philadelphia, PA) for helpful discussions and comments on earlier versions of the manuscript, D. Colman (Mount Sinai School of Medicine, New York), E. Hertzberg (Albert Einstein College of Medicine, Bronx, NY), and J. Salzer (New York University School of Medicine, New York) for the antibodies against E-cadherin, Cx32, and MAG, and especially K. Willecke for *cx32*-null mice.

This work was supported by grants from the National Institutes of Health to R. Balice-Gordon (NS-34373), and S.S. Scherer, K. Fischbeck, and R. Balice-Gordon (NS-08075), the Muscular Dystrophy Association to K. Fischbeck and S.S. Scherer (97-010), a McKnight Neuroscience Scholar award to R. Balice-Gordon, and a Murray M. Stokely Award from the American Academy of Neurology to S.S. Scherer. L.J. Bone was supported by the Medical Scientist Training Program and was a graduate student in the Cell and Molecular Biology graduate group.

Received for publication 10 April 1998 and in revised form 18 June 1998.

References

Anzini, P., D.H.-H. Neuberg, M. Schachner, E. Nelles, K. Willecke, J. Zielasek, K. Toyka, U. Suter, and R. Martini. 1997. Structural abnormalities and deficient maintenance of peripheral nerve myelin in mice lacking the gap junc-

tion protein connexin32. *J. Neurosci.* 17:4545–4561.
Balice-Gordon, R.J. 1998. In vivo approaches to neuromuscular junction structure and function. *In* Methods in Cell Biology. C.P. Emerson and H.L. Sweeney, editors. Academic Press, San Diego, CA. 323–348.
Berg, H.C. 1983. Random Walks in Biology. Princeton University Press, Princeton, NJ. 142 pp.
Bergoffen, J., S.S. Scherer, S. Wang, M. Oronzi-Scott, L. Bone, D.L. Paul, K. Chen, M.W. Lensch, P. Chance, and K. Fischbeck. 1993. Connexin mutations in X-linked Charcot-Marie-Tooth disease. *Science.* 262:2039–2042.
Berthold, C.-H., and M. Rydmark. 1995. Morphology of normal peripheral axons. *In* The Axon. S.G. Waxman, J.D. Kocsis, and P.K. Stys, editors. Oxford University Press, New York. 13–48.
Bone, L.J., S.M. Deschênes, R.J. Balice-Gordon, K.H. Fischbeck, and S.S. Scherer. 1997. Connexin32 and X-linked Charcot-Marie-Tooth disease. *Neurobiol. Dis.* 4:221–230.
Bruzzone, R., T.W. White, and D.L. Paul. 1996. Connections with connexins: the molecular basis of direct intercellular signaling. *Eur. J. Biochem.* 238:1–27.
Chandross, K.J., J.A. Kessler, R.I. Cohen, E. Simburger, D.C. Spray, P. Bieri, and R. Dermietzel. 1996*a*. Altered connexin expression after peripheral nerve injury. *Mol. Cell. Neurosci.* 7:501–518.
Chandross, K.J., D.C. Spray, R.I. Cohen, N.M. Kumar, M. Kremer, R. Dermietzel, and J.A. Kessler. 1996*b*. TNFα inhibits Schwann cell proliferation, connexin46 expression, and gap junctional communication. *Mol. Cell. Neurosci.* 7:479–500.
Chiu, S.Y. 1991. Functions and distribution of voltage-gated sodium and potassium channels in mammalian Schwann cells. *Glia.* 4:541–558.
Claude, P., and D.A. Goodenough. 1973. Fracture faces of zonulae occludentes from "tight" and "leak" epithelia. *J. Cell Biol.* 58:390–400.
David, G., J.N. Barrett, and E.F. Barrett. 1993. Activation of internodal potassium conductance in rat myelinated axons. *J. Physiol.* 472:177–202.
Davidson, J.S., and I.M. Baumgarten. 1988. Glycyrrhetinic acid derivatives: a novel class of inhibitors of gap-junctional intercellular communication. Structure-activity relationships. *J. Pharm. Exp. Therap.* 246:1104–1107.
Dezawa, M., T. Mutoh, A. Dezawa, and E. Adachi-Usami. 1998. Putative gap junctional communication between axon and regenerating Schwann cells during mammalian peripheral nerve regeneration. *Neuroscience.* 85:663–667.
Elfgang, C., R. Eckert, H. Lichternberg-Frate, A. Butterweck, O. Traub, R.A. Klein, D.F. Hulser, and K. Willecke. 1995. Specific permeability and selective formation of gap junction channels in connexin-transfected HeLa cells. *J. Cell Biol.* 129:805–817.
Fannon, A.M., D.L. Sherman, G. Ilyina-Gragerova, P.J. Brophy, V.L. Friedrich, and D.R. Colman. 1995. Novel E-cadherin mediated adhesion in peripheral nerve: Schwann cell architecture is stabilized by autotypic adherens junctions. *J. Cell Biol.* 129:189–202.
Friede, R.L., and R. Bischhausen. 1980. The precise geometry of large internodes. *J. Neurol. Sci.* 48:367–381.
Friend, D.S., and N.B. Gilula. 1972. Variation in tight and gap junctions in mammalian tissues. *J. Cell Biol.* 53:758–776.
Goldberg, G.S., A.P. Moreno, J.F. Bechberger, S.S. Hearn, R.R. Shivers, D.J. MacPhee, Y.-C. Zhang, and C.C.G. Naus. 1996. Evidence that disruption of connexon particle arrangements in gap junction plaques is associated with inhibition of gap junctional communication by a glycorrhetinic acid derivative. *Exp. Cell Res.* 222:48–53.
Goodenough, D.A., J.A. Goliger, and D.L. Paul. 1996. Connexins, connexons, and intercellular communication. *Annu. Rev. Biochem.* 65:475–502.
Gould, R.M., and G. Mattingly. 1990. Regional localization of RNA and protein metabolism in Schwann cells in vivo. *J. Neurocytol.* 19:285–301.
Hahn, A.F., W.F. Brown, W.J. Koopman, and T.E. Feasby. 1990. X-linked dominant hereditary motor and sensory neuropathy. *Brain.* 113:1511–1525.
Herr, J.C., and P.M.J. Heidger. 1978. A freeze-fracture study of exocytosis and reflexive gap junctions in human ovarian decidual cells. *Am. J. Anat.* 152:29–44.
Konishi, T. 1990. Dye coupling between mouse Schwann cells. *Brain Res.* 508: 85–92.
Lev-Ram, V., and M.H. Ellisman. 1995. Axonal activation-induced calcium transients in myelinating Schwann cells, sources, and mechanisms. *J. Neurosci.* 15:2628–2637.
Li, J., E.L. Hertzberg, and J.I. Nagy. 1997. Connexin32 in oligodendrocytes and association with myelinated fibers in mouse and rat brain. *J. Comp. Neurol.* 379:571–591.
Majack, R.A., and W.J. Larsen. 1980. The bicellular and reflexive membrane junctions of renomedullary interstitial cells: functional implications of reflexive gap junctions. *Am. J. Anat.* 157:181–189.
Mi, H.Y., T.J. Deerinck, M.H. Ellisman, and T.L. Schwarz. 1995. Differential distribution of closely related potassium channels in rat Schwann cells. *J. Neurosci.* 15:3761–3774.
Mi, H.Y., T.J. Deerinck, M. Jones, M.H. Ellisman, and T.L. Schwarz. 1996. Inwardly rectifying K^+ channels that may participate in K^+ buffering are localized in microvilli of Schwann cells. *J. Neurosci.* 16:2421–2429.
Mugnaini, E., K.K. Osen, B. Schnapp, and V.L. Friedrich, Jr. 1977. Distribution of Schwann cell cytoplasm and plasmalemmal vesicles (caveole) in peripheral myelin sheaths. An electron microscopic study with thin sections and freeze-fracturing. *J. Neurocytol.* 6:647–668.
Nelles, E., C. Butzler, D. Jung, A. Temme, H.-D. Gabriel, U. Dahl, O. Traub, F. Stumpel, K. Jungermann, J. Zielasek, et al. 1996. Defective propagation of signals generated by sympathetic nerve stimulation in the liver of connexin32-deficient mice. *Proc. Natl. Acad. Sci. USA.* 93:9565–9570.
Orkand, P.M., J.G. Nicholls, and S.W. Kuffler. 1966. Effect of nerve impulses on the membrane potential of glial cells in the central nervous sytem of amphibia. *J. Neurophysiol.* 29:788–806.
Pedraza, L., G.C. Owens, L.A.D. Green, and J.L. Salzer. 1990. The myelin-associated glycoproteins: membrane disposition, evidence of a novel disulfide linkage between immunoglobulin-like domains, and posttranslational palmitylation. *J. Cell Biol.* 111:2651–2661.
Reynolds, M.L., and C.J. Woolf. 1992. Terminal Schwann cells elaborate extensive processes following denervation of the motor endplate. *J. Neurocytol.* 21:50–66.
Rozear, M.P., M.A. Pericak-Vance, K. Fischbeck, J.M. Stajich, P.C. Gaskell, Jr., D.A. Krendel, D.G. Graham, D.V. Dawson, and A.D. Roses. 1987. Hereditary motor and sensory neuropathy, X-linked: a half century follow-up. *Neurology.* 37:1460–1465.
Rumessen, J.J., L. Thuneberg, and B. Mikkelsen. 1982. Plexus muscularis profundus and associated interstitial cells. II. Ultrastructural studies of mouse small intestine. *Anat. Rec.* 203:129–146.
Salzer, J.L. 1997. Clustering sodium channels at the node of Ranvier: Close encounters of the axon-glia kind. *Neuron.* 18:843–846.
Sander, S., G.A. Nicholson, R.A. Ouvrier, J.G. McLeod, and J.D. Pollard. 1998. Charcot-Marie-Tooth disease: histopathological features of the peripheral myelin protein (PMP22) duplication (CMT1A) and connexin32 mutations (CMTX1). *Muscle Nerve.* 21:217–225.
Sandri, C., J.M. Van Buren, and K. Akert. 1982. Membrane morphology of the vertebrate nervous system. *Prog. Brain Res.* 46:201–265.
Scherer, S.S. 1996. Molecular specializations at nodes and paranodes in peripheral nerve. *Microsc. Res. Tech.* 34:452–461.
Scherer, S.S., S.M. Deschênes, Y.-T. Xu, J.B. Grinspan, K.H. Fischbeck, and D.L. Paul. 1995. Connexin32 is a myelin-related protein in the PNS and CNS. *J. Neurosci.* 15:8281–8294.
Scherer, S.S., Y.-T. Xu, E. Nelles, K. Fischbeck, K. Willecke, and L.J. Bone. 1998. Connexin32-null mice develop a demyelinating peripheral neuropathy. Glia. 24:8–20.
Shinowara, N.L., W.B. Beutel, and J.-P. Revel. 1980. Comparative analysis of junctions in the myelin sheath of central and peripheral axons of fish, amphibians and mammals: a freeze-fracture study using complementary replicas. *J. Neurocytol.* 9:15–38.
Son, Y.-J., and W.J. Thompson. 1995*a*. Nerve sprouting in muscle is induced and guided by processes extended by Schwann cells. *Neuron.* 14:133–141.
Son, Y.-J., and W.J. Thompson. 1995*b*. Schwann cell processes guide regeneration of peripheral axons. *Neuron.* 14:125–132.
Sontheimer, H. 1994. Voltage-dependent ion channels in glial cells. *Glia.* 11: 156–172.
Stolinski, C., and A.S. Breathnach. 1982. Freeze-fracture replication of mammalian peripheral nerve —a review. *J. Neurol. Sci.* 57:1–28.
Tetzlaff, W. 1978. The development of a zonula occludens in peripheral myelin of the chick embryo. *Cell Tiss. Res.* 189:187–201.
Tetzlaff, W. 1982. Tight junction contact events and temporary gap junctions in the sciatic nerve fibres of the chicken during Wallerian degeneration and subsequent regeneration. *J. Neurocytol.* 11:839–858.
Wilson, G.F., and S.Y. Chiu. 1993. Mitogenic factors regulate ion channels in Schwann cells cultured from newborn rat sciatic nerve. *J. Physiol.* 470:501–520.
Yoshimura, T., M. Satake, and T. Kobayashi. 1996. Connexin43 is another gap junction protein in the peripheral nervous system. *J. Neurochem.* 67:1252–1258.